

See discussions, stats, and author profiles for this publication at: <https://www.researchgate.net/publication/261747641>

Dearomative Indole (3+2) Cycloaddition Reactions

ARTICLE in JOURNAL OF THE AMERICAN CHEMICAL SOCIETY · APRIL 2014

Impact Factor: 12.11 · DOI: 10.1021/ja412435b · Source: PubMed

CITATIONS

26

READS

92

3 AUTHORS:



Hui Li

Dartmouth College

11 PUBLICATIONS 78 CITATIONS

SEE PROFILE



Russell P Hughes

Dartmouth College

236 PUBLICATIONS 4,036 CITATIONS

SEE PROFILE



Jimmy Wu

Dartmouth College

51 PUBLICATIONS 1,082 CITATIONS

SEE PROFILE

Dearomative Indole (3 + 2) Cycloaddition Reactions

Hui Li, Russell P. Hughes,* and Jimmy Wu*

Department of Chemistry, Dartmouth College, Hanover, New Hampshire 03755, United States

S Supporting Information

ABSTRACT: A diastereoselective (3 + 2) dearomative annulation of 3-substituted indoles with α -haloketones has been developed. Significant regiochemical control was observed. This methodology provides easy access to highly functionalized cyclopenta- or cyclohexa-fused indoline compounds, which are common structures of many natural products. The synthetic potential of this reaction was demonstrated in the concise syntheses of the core structures of vincorine, isocorymine, and aspidophylline A. DFT studies (B3LYP-D3/6-311++G**/MeOH) on cyclization mechanisms involving the 2-hydroxyallyl cation and its deprotonated oxyallyl cation have been performed. Under the reaction conditions, with a sparingly soluble Na_2CO_3 base, both species may be present and both pathways are viable. Both pathways support the formation of the experimentally observed *O*-bound intermediate, its transformation to the final product, the regiochemical and eventual stereochemical outcome of the kinetic cyclization product, and the thermodynamic preference for formation of the final stereoisomer.



INTRODUCTION

Dearomatization of indoles has been a powerful strategy for organic chemists to access many architecturally complex alkaloids.¹ Due to the ubiquitous nature of the indole unit in important bioactive alkaloids, numerous chemo-, regio-, and enantioselective methodologies have emerged. Some dearomatization strategies include allylation,² alkylation,³ arylation,⁴ iminium catalysis,⁵ and cycloaddition.⁶ Dearomative cycloaddition, which is based on the reactivity of the C2=C3 double bond of indole, is an attractive and straightforward approach to fused indoline compounds. Moreover, indolines with a fused five- or six-membered ring at the C2 and C3 positions are well represented in nature (Figure 1).⁷

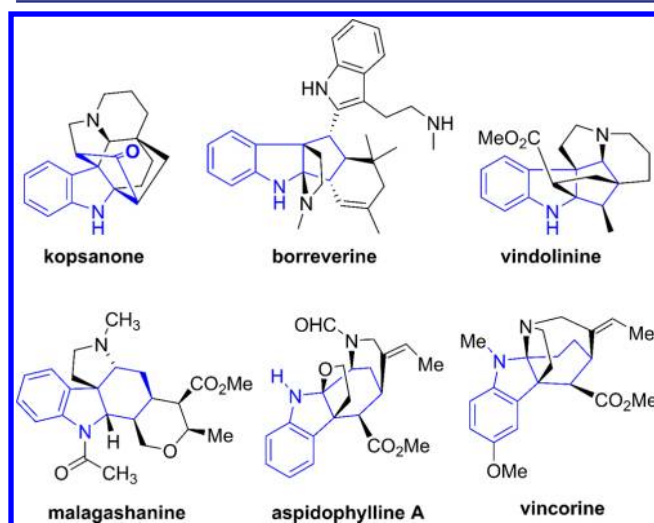


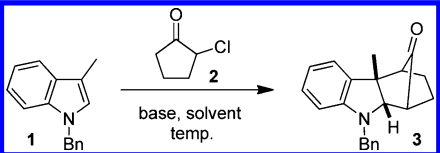
Figure 1. Natural products with fused five- and six-membered rings.

Indoles have been shown to undergo (4 + 2) cycloaddition reactions to afford hydrocarbazoles.^{6c,d,8} Nevertheless, only limited reports are available on dearomative (3 + 2) cycloaddition of indoles.⁹ Kerr and Pagenkopf have reported Lewis acid catalyzed C2/C3 cyclopentannulation of indole with 1,1-cyclopropane diesters and 2-methoxy-1-cyclopropane esters, respectively.^{9a,b} Recently, Tang and co-workers developed a copper-catalyzed enantioselective version.^{9c} Barluenga and co-workers have reported an enantioselective (3 + 2) cycloaddition reaction of indole with alkynyl Fischer carbenes,^{9d} while Lian and Davies established a rhodium-catalyzed variant with vinyl diazoacetates.^{9e} The examples above indicate that the use of 1,3-dipoles to dearomatize the C2=C3 double bond of indole and its derivatives can be a successful strategy to synthesize cyclopentannulated indolines.

1,3-Dipoles have been of particular interest to us because, for some time, our group has been developing annulation and alkylation reactions of indole and related heterocycles.^{10,11} In particular, the oxyallyl cation dipole usually reacts with dienes to furnish seven-membered rings.¹² However, they have also been shown to undergo simple alkylation reactions¹³ as well as (3 + 2) cycloadditions with allylsilanes,¹⁴ dienes,¹⁵ furans,¹⁶ and enamines.¹⁷ Nonetheless, little is known about its reactivity in dearomatization processes with substituted indoles. We envisioned that oxyallyl or hydroxyallyl cations generated *in situ* from α -haloketones may undergo formal dearomative (3 + 2) cycloaddition with indoles. Herein, we describe our progress in this subject matter.

Received: December 6, 2013

Published: April 17, 2014

Table 1. Optimization of Reaction Conditions^a


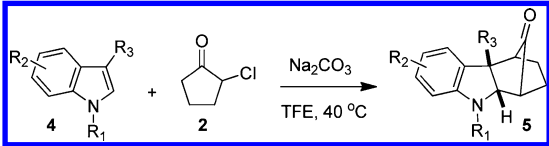
entry	base	solvent	concn (M)	temp (°C)	time (h)	yield ^b % (brsm) ^c	dr ^d
1	Na ₂ CO ₃	MeOH/H ₂ O ^f	0.2	rt	24	5 (73)	N/A ^e
2	Na ₂ CO ₃	DMSO	0.2	rt	24	3 (82)	N/A ^e
3	NaOH	MeOH	0.2	rt	24	15 (75)	N/A ^e
4	NaOH	MeOH/H ₂ O ^f	0.2	rt	24	14 (73)	N/A ^e
5	Na ₂ CO ₃	MeOH	0.5	rt	24	23 (80)	12:1
6	Na ₂ CO ₃	TFE	0.5	rt	24	71 (95)	6:1
7	Na ₂ CO ₃	TFE	1	rt	24	79 (88)	5:1
8	Et ₃ N	TFE	1	rt	6.5	48 (48)	4.6:1
9	DIPEA	TFE	1	rt	17	71 (71)	6.7:1
10	DMAP	TFE	1	rt	11	51 (51)	4.6:1
11	Na ₂ CO ₃	TFE	1	40	10	93 (93)	6:1

^aIndole (1 equiv), 2-chlorocyclopentanone (1.4 equiv), and base (1.5 equiv). ^bIsolated yield. ^cYield based on recovered starting material.^dDetermined by ¹H NMR analysis of unpurified product. ^eNot determined. ^f1:1 v/v.

RESULTS AND DISCUSSION

We initiated our study by examining the reaction between *N*-benzylskatole (**1**) and 2-chlorocyclopentanone **2** (Table 1). Little product was obtained after 24 h using Na₂CO₃ in a mixture of MeOH/H₂O or DMSO (entries 1 and 2). The use of stronger inorganic bases such as NaOH in MeOH or MeOH/H₂O did not accelerate the reaction either and still gave low yields after 24 h (entries 3 and 4). Inspired by the reports of Chi, MacMillan, and Harmata,^{12a,13} trifluoroethanol (TFE) was investigated as a solvent. Its use substantially increased the reaction rate (entries 5 and 6). This is likely because, as compared to MeOH, TFE is a stronger H-bond donor and, hence, can more effectively promote enolate formation/enolization as well as weaken the C–Cl bond. Higher concentrations of the reactants also accelerated the reaction (entries 6 and 7). We then investigated three organic bases: Et₃N, DIPEA, and DMAP (entries 8, 9, and 10), which shortened the reaction time but furnished poorer yields. The best yield and reactivity were obtained by conducting the reaction in TFE (1 M) at 40 °C (entry 11).

With the optimized conditions in hand, we explored the reaction scope between 2-chlorocyclopentanone (**2**) and various 3-substituted indoles **4** (Table 2). The reaction worked well, affording good to excellent yields and diastereoselectivities. Electron-rich indoles (Table 2, entry 10) tended to accelerate the reaction, while indoles with a relatively strong electron-withdrawing group (5-CO₂Me) appeared unreactive. This reaction was tolerant to different C3 substituents on indole other than methyl, thus allowing additional functionalities such as silyl ether, amino, allyl, and iodo groups to be introduced into the products (Table 2, entries 6–10, 15). Both the hydroxyl and amino groups needed to be protected so that they would not act as nucleophiles and interrupt the (3 + 2) cycloaddition. That the pendant iodine in entry 15 (Table 2) was not destroyed is a testament to the mildness of the reaction. C2-,C3-disubstituted indoles were not compatible with the reaction when using **2**; however, acyclic chloroketones are amenable to cyclization with indoles possessing this substitution pattern (*vide infra*). We have also examined the reactivity of *N*-H and *N*-protected indoles. For instance, *N*-

Table 2. Cycloaddition Reactions of 3-Substituted Indoles with 2-Chlorocyclopentanone^{a,b}


Entry	R ₁	R ₂	R ₃	Yield ^c (%)	dr ^d	t (h)
1	Bn	H	<i>i</i> -Pr	87	11:1	20
2	Bn	H	cyclohexyl	84	18:1	23
3	Bn	H	<i>p</i> -MeOBn	71	17:1	14
4	Bn	5-Cl	<i>i</i> -Pr	91	32:1	31
5	Bn	5-I	<i>i</i> -Pr	92	27:1	47
6	Bn	H	allyl	83	11:1	22
7	Bn	H	TBSO-CH ₂ CH ₂ -	82	14:1	24
8	Bn	H	TBSO-CH ₂ CH ₂ -CH ₂ -	74	13:1	30
9	Bn	H	PhthN-CH ₂ CH ₂ -	87	10:1	23
10	Bn	5-OMe	PhthN-CH ₂ CH ₂ -	83	8.7:1	11
11	Me	H	Me	91	5:1	11
12	Me	5-Br	Me	88	4.5:1	20
13	Me	H	<i>p</i> -MeOBn	71	17:1	14
14	Me	H	cyclohexyl	82	16:1	22
15	Me	H	I-CH ₂ CH ₂ -	88	4.5:1	19
16	allyl	H	Me	79	7.5:1	15
17 ^e	<i>i</i> -Pr	H	<i>p</i> -FPh	79	1.5:1	43

^aIndole (1 equiv), 2-chlorocyclopentanone (1.4 equiv) and Na₂CO₃ (1.5 equiv) in TFE. ^bReaction concentration was 1 M. ^cIsolated yield.^dDetermined by ¹H NMR. ^eTotal of 2.1 equiv of 2-chlorocyclopentanone used.

methyl, -Bn, -allyl, and -*i*Pr indoles worked well, but neither *N*-H nor *N*-Cbz protected indoles were suitable substrates. For

the products in entries 1 and 11 (Table 2), the relative stereochemical configuration of each diastereomer was established by NOESY experiments (Figure 2). The relative stereochemistries of the remaining products were assigned by analogy.

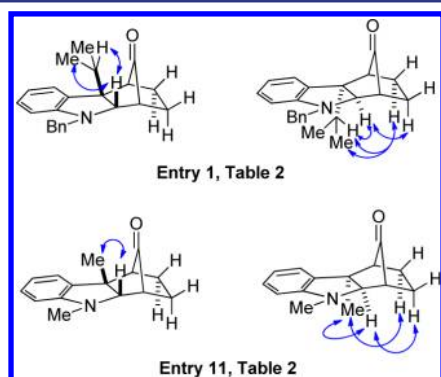
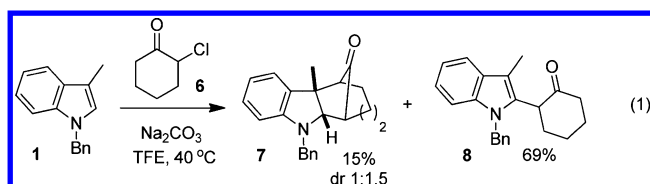


Figure 2. Selected NOESY data for diastereomers in Table 2.

Attempts to extend the scope of cyclic α -haloketone to include 2-chlorocyclohexanone and 2-chlorocycloheptanone were unsuccessful. The latter was unreactive to *N*-benzylskatole; the former furnished poor yields of the desired product **7** (eq 1) while affording mostly C2 alkylated product **8**,



presumably arising from 1,2-migration of a C3 alkylated intermediate followed by aromatization. When both minor and major isomers of **7** were purified and resubjected to the reaction conditions, fragmentation to **8** did not occur, thereby precluding the possibility that **8** is derived from **7**.

The scope and generality of this cycloaddition in terms of indole substitution with acyclic α -haloketones are summarized in Table 3. Unlike the reaction with 2-chlorocyclopentanone (**2**), C2,C3-disubstituted indoles were indeed compatible to annulation using acyclic haloketones (Table 3, entries 1 and 2). However, longer reaction times and, in some cases, higher temperatures (Table 3, entries 1–4) were required. The employment of electron-rich indole **11** (Table 3, entry 4) did not accelerate the reaction relative to entry 3. Instead, elevated temperatures were required to drive the reaction to completion. This is likely due to the bulkier isopropyl group of **11**. These results also show that the (3 + 2) cycloadditions proceeded with excellent regio- and diastereoselectivities. Single regioisomers were isolated for entries 1–4. Similar results were observed for α -haloketones **14**–**17** (Table 3, entries 6–9), which also furnished their respective products as single regioisomers. Moreover, compound **23** was formed in high diastereoselectivities relative to the substituent on the α -haloketone fragment (>20:1 of **23**:**24**).

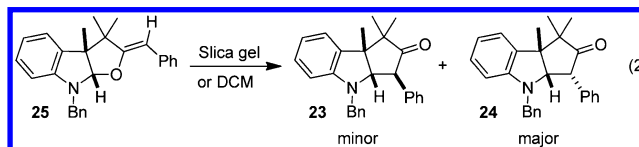
It is noteworthy that, for entries 6–9, a common *O*-alkylated intermediate **25** was isolated and confirmed by NMR analysis, suggesting the possibility that α -haloketones **14**–**17** may proceed via the same oxyallyl or hydroxyallyl intermediate. We also discovered that the rearrangement of **25** to a mixture

Table 3. Cycloaddition Reactions of 3-Substituted Indoles with Acyclic α -Haloketones^{a,b}

Entry	Indoles	α -Haloketone	Product	Yield ^c (%)	dr ^d	t (h)
1				81 ^{e,f}	N/A	43
2		12		77 ^{e,f,g}	N/A	75
3		12		76 ^{e,f}	N/A	90
4		12		72 ^{f,h}	N/A	45
5	1			47 ⁱ	ND ^j	40
6	1		 23 (major) + 24 (minor)	50 ^{k,l}	>20:1	9 d
7	1			46 ^{k,m}	>20:1	9 d
8	1			71 ^k	>20:1	49
9	1			74 ^k	>20:1	49

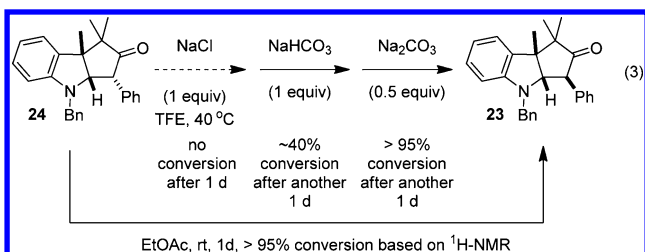
^aIndole (1 equiv) and Na₂CO₃ (1.5 equiv) in TFE. ^bReaction concentration was 1.0 M. ^cIsolated yield. ^dAs determined by ¹H NMR spectroscopy. ^e50 °C. ^f2.0 equiv of α -haloketones **12** used. ^g95% brsm. ^h75 °C. ⁱ1.4 equiv of α -haloketones **12** used. ^jNot determined. ^k α -haloketones (2.0 equiv) Na₂CO₃ (2.2 equiv). ^l58% brsm. ^m59% brsm.

of **23** (minor diastereomer) and **24** (major diastereomer) occurred upon treatment with silica gel or prolonged standing in CH₂Cl₂ (eq 2).



However, in contrast to results shown in eq 2, **23** was invariably the major diastereomer isolated in the overall reactions for entries 6–9. In order to explain these results, we performed stability experiments on diastereomer **24**. We discovered that a mixture of **24** and NaCl in TFE did not epimerize to **23**, while such epimerization was observed upon

treatment with bicarbonate or carbonate base (eq 3). We also discovered that simply dissolving **24** in EtOAc results in its



conversion to **23** over the course of 1 day (eq 3). These data suggest that compound **23** is likely the thermodynamically preferred diastereomer while **24** is the kinetically favored one.

For entries 2, 3, 5–9 (Table 3) regio- and stereochemical assignments were established by extensive NMR analyses, including DEPT, HMBC, HMQC, and NOESY. The regio- and stereochemistry of the products in entries 1 and 4 (Table 3) were assigned by analogy. Further structural confirmation of **23** was established by single crystal X-ray analysis (Figure 3).

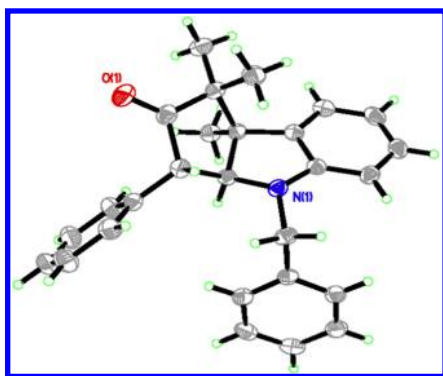


Figure 3. X-ray structure of compound **23**.

In order to gain more detailed mechanistic information regarding these (3 + 2) cycloaddition reactions, kinetic experiments on the reactions for entries 7 and 9 (Table 3) were carried out. As shown in Figure 4, they both behaved similarly with respect to the generation of minor diastereomer **24** (purple line), which was steadily formed throughout both reactions. The most prominent difference between the kinetic profiles is that with the use of **17**, there is a significant buildup of the *O*-alkylated intermediate **25** (Figure 4b; red line) during the first 20 h, whereas, with α -haloketone **15**, the level of **25** remained low (Figure 4a). We believe this difference reflects a change in the rate-determining step (discussion to follow). A second significant dissimilarity is that the reaction rate with **15** was much slower as compared to that of **17**. This was deduced by comparing their consumption of *N*-benzylskatole (**1**) and/or formation of product **23**.

Scheme 1 illustrates our proposed mechanism for the (3 + 2) cycloaddition. The reduced acidity of the α -proton of **15** (i.e., higher pK_a) as compared to that of **17** makes **15** more resistant to enolization. Moreover, the kinetic acidity of **15** may also be low as a result of the stereoelectronic demands required for enolization/tautomerization (i.e., α -proton needs to be coplanar with the carbonyl π -system). If the activation energy of enolization for **15** were high enough to render this step rate-determining, this would be consistent with the lack of an

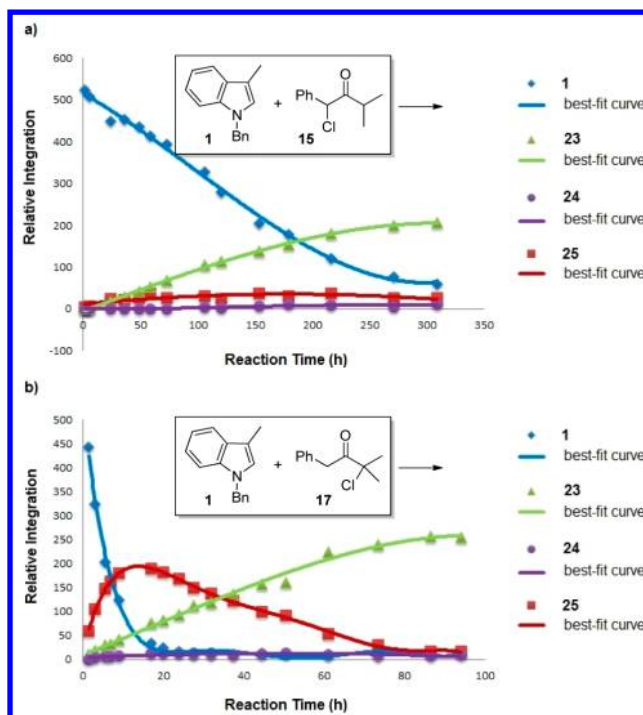
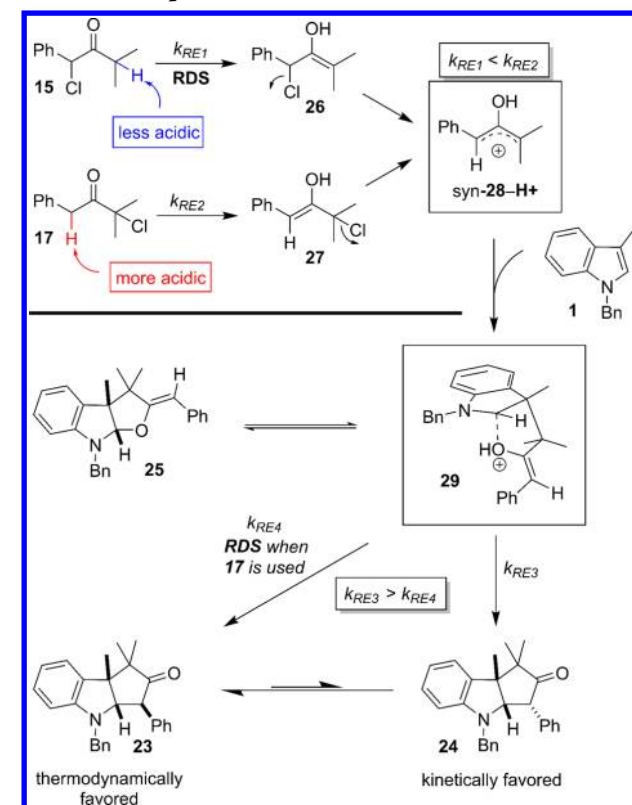


Figure 4. (a) Kinetic profile of reaction for entry 7, Table 3. (b) Kinetic profile of reaction for entry 9, Table 3. (All reactions were monitored by ^1H -NMR spectroscopy using hexamethyl benzene as an internal standard).

Scheme 1. Proposed Reaction Mechanism



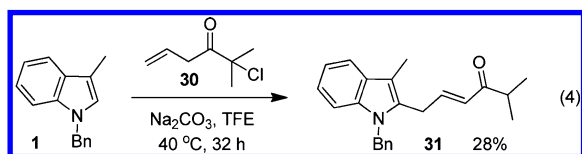
observed buildup of any intermediates along the pathway toward product when using **15**.

In contrast, we believe that enolization of **17** to give **27** (k_{RE2}) is fast relative to k_{RE1} . This would be followed by

chloride ionization (aided by H-bonding with TFE) to generate hydroxyallyl cation *syn*-**28-H**⁺. While other cycloaddition reactions are thought to proceed through *enolate* oxyallyl cations,¹² DFT calculations on our system suggest that a route via hydroxyallyl cation *syn*-**28-H**⁺ may also be available under the reaction conditions (*vide infra*). In this scenario, *N*-benzylskatole (**1**) then attacks *syn*-**28-H**⁺ to form intermediate **29** which possesses a weak C⋯OH interaction. Harmata, Schreiner, and co-workers have also reported a divergence in reactivity between oxyallyl and hydroxyallyl cations.¹⁸ Removal of the proton with the carbonate base at this point would furnish the observed intermediate **25**. Alternatively, the protonated form **29** can redissociate and alkylate at carbon to generate the kinetic cycloadduct **24**, which can then isomerize to the thermodynamic product **23**. We believe that when using α -haloketone **17**, the overall transformation **29** \rightarrow **24** and then to **23** is rate-determining. The observed buildup of **25** is consistent with its formation prior to the RDS when **17** is used.

As described above, diastereomer **24** is the kinetically favored product, but, under the reaction conditions, it epimerizes to the more thermodynamically favored isomer **23**. Our present use of a good H-bonding solvent (TFE), in combination with a weak non-nucleophilic base (Na₂CO₃), to generate oxyallyl and hydroxyallyl cations by means of soft enolization has been previously reported by MacMillan and Chi.¹³

Attempts to employ compound **30** as a substrate was unsuccessful. What we obtained was alkylation at C2 (eq 4). Transposition of the double bond supports the intermediacy of a hydroxyallyl cation species.



Applications toward Natural Products. We have also investigated the potential utility of using the title reaction in the syntheses of several indoline-containing alkaloids. In this regard, we have prepared the core structures of vincorine,^{7f–h} isocorymine,¹⁹ and aspidophylline A (Figure 5).^{7e,i}

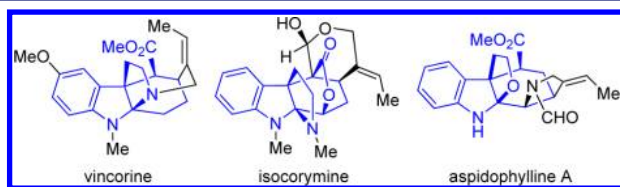
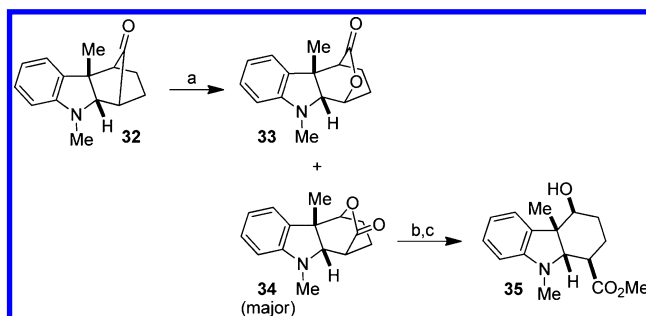


Figure 5. Structures of vincorine, isocorymine, and aspidophylline A (*n.b.*, drawn as their enantiomers).

As shown in Scheme 2, ketone **32** was subjected to Baeyer–Villiger oxidation using *m*-cpba to afford lactone **34** as the major regioisomer (3:1 mixture). Hydrolysis of **34** under alkaline conditions, followed by esterification, furnished cyclohexa-fused indoline **35**.

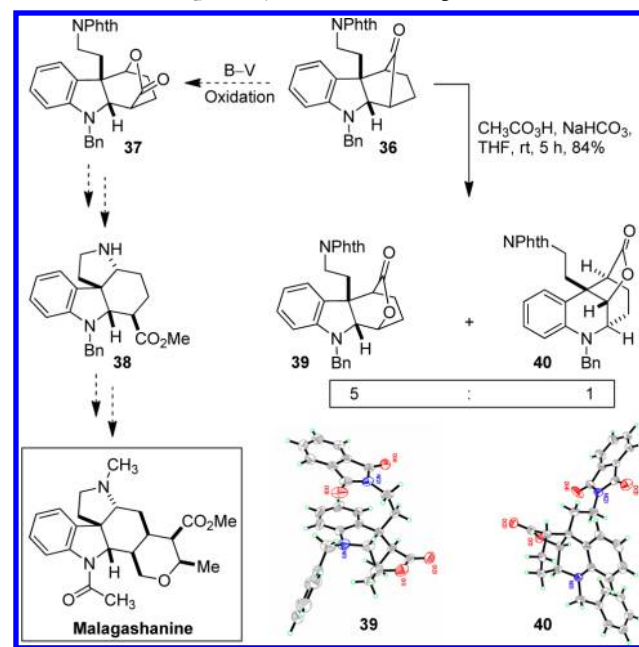
We hypothesized that an analogous regioselective oxidation of **36** could afford lactone **37**, a promising precursor to malagashanine (Scheme 3). We first examined the oxidation of **36** with *m*-cpba in THF at rt. The reaction turned out to be very sluggish. Other oxidants such as H₂O₂ or *t*-BuOOH did not perform well either. Finally, we identified peracetic acid as

Scheme 2. Baeyer–Villiger Oxidation^a



^a(a) *m*-CPBA, NaHCO₃, **33**:**34** (1:3), 81% combined yield; (b) NaOH, MeOH/H₂O, rt, 1 h; (c) MeI, K₂CO₃, DMF, 20 min, rt, 90% over two steps.

Scheme 3. Attempted Synthesis of Malagashanine Core

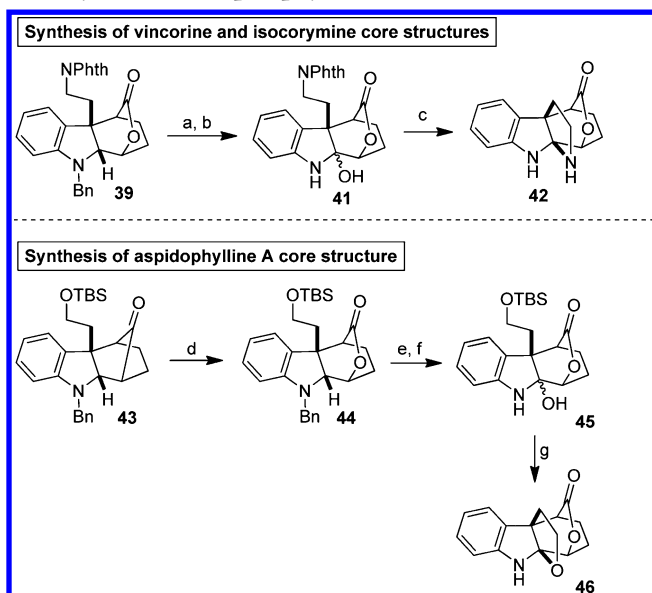


an efficient oxidant in which two lactones were isolated in a 5:1 ratio and a combined yield of 84%. However, neither of the lactones turned out to be **37**. The major product was the undesired regioisomer **39**, while the other was rearranged lactone **40**. The structures of both **39** and **40** have been confirmed by single crystal X-ray analysis.

Although Baeyer–Villiger oxidation of compound **36** failed to provide lactone **37**, we investigated potential applications for its regioisomer **39**. Scheme 4 illustrates three short syntheses of the core structures of vincorine, isocorymine, and aspidophylline A. Debenzylation of lactone **39** by hydrogenolysis and subsequent oxidation with Dess–Martin periodinane (DMP) led to hemiaminal **41**. Cleavage of the phthalimide group with MeNH₂ liberated the free amine, which was followed by spontaneous ring closure to install the pyrrolidine ring of pentacycle **42**. Compound **42** maps well to vincorine and isocorymine. By employing a similar strategy, pentacycle **46** was obtained from **43**, providing a good starting point for the synthesis of aspidophylline A.

Computational Studies. DFT studies were carried out using the B3LYP-D3 functional²⁰ and the 6-311++G** basis set,²¹ as implemented in the Jaguar²² suite of programs. This

Scheme 4. Synthesis of Core Structures for Vincorine, Isocorymine, and Aspidophylline A^a



^a(a) Pd(OH)₂, EtOAc, H₂, rt, overnight; (b) DMP, CH₂Cl₂, rt, 0.5 h, 82% for two steps; (c) MeNH₂, MeOH, rt, overnight, 81%; (d) CH₃CO₃H, NaHCO₃, THF, rt, overnight, 61%; (e) Pd/C, EtOAc, H₂, rt, overnight; (f) DMP, CH₂Cl₂, rt, 1 h, 90% for two steps; (g) *p*-TSA (cat.), toluene, reflux, 3 h, 99%.

dispersion corrected functional²³ has proven to be essential in modeling other cyclization reactions of indoles and especially in assessing activation parameters for similar two-component additions for which intermolecular dispersion interactions are crucial components of the overall transition state energetics.²⁴ A Poisson–Boltzmann solvation model²⁵ as implemented in Jaguar was applied using methanol as the solvent. The chosen DFT method and basis perform well in predicting structures of this type; a superimposition of the calculated and X-ray structures of **23** is shown in Figure 6.

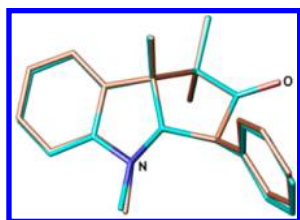


Figure 6. Superimposition of X-ray structure (bronze) of compound **23** with that calculated by DFT (B3LYP-D3/6-311++G**) for its *N*-methyl analogue (blue). H's are omitted for clarity.

The key intermediate derived from either haloketone must be the oxyallyl cation *syn*/*anti*-**28** or its *O*-protonated form *syn*/*anti*-**28-H**⁺. We recognize the option that **28** might also be a singlet diradical, as discussed for the unsubstituted parent system.²⁶ Our own calculations (UDFT/B3LYP-D3/6-311++G**) confirm that the *parent* species does converge to a singlet diradical structure. However, **28** invariably converges to a closed-shell structure, which was used as the basis for further calculations. We have also attempted to address whether **28** or its protonated form **28-H**⁺ is present under the reaction conditions (*vide infra*). Deprotonation of **28-H**⁺ requires a base that could be either the solvent or the added base

(CO₃²⁻). Free energies of the optimized *syn*- and *anti*-isomers of **28** and **28-H**⁺ were calculated in a methanol solvent, and relative values are shown in Figure 7. As expected, the *syn*-

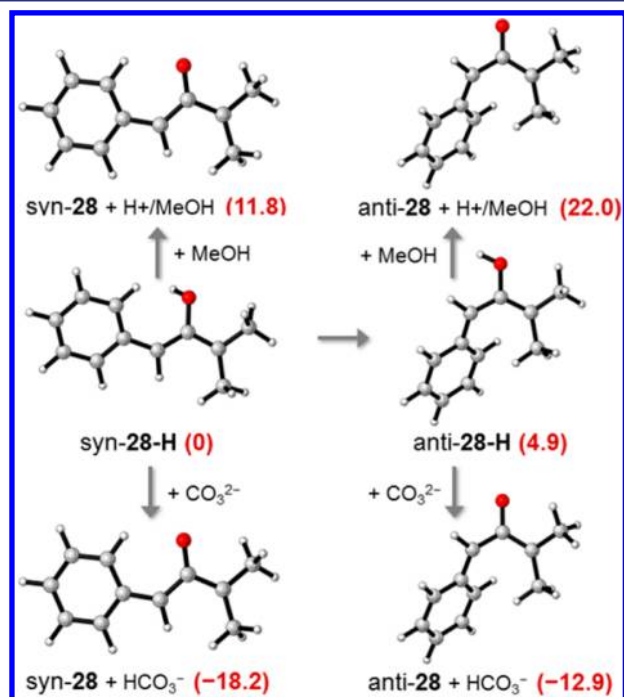


Figure 7. DFT calculated (B3LYP-D3/6-311++G**/CH₃OH) structures for *syn* and *anti* isomers of hydroxyallyl cation **28-H**⁺ and their deprotonation by solvent (MeOH) or base (CO₃²⁻) to give *syn* and *anti* isomers of oxyallyl cation **28**. Relative free energies (kcal/mol) are in red.

isomer is, in each case, significantly more stable than its *anti*-analogue. Comparison of the ΔG values for deprotonation of *syn*- and *anti*-**28-H**⁺ to give their deprotonated analogues **28** were made using solvent (MeOH) or solubilized CO₃²⁻ as bases; the computationally derived absolute free energy of the proton in methanol (−263.5 kcal/mol) was used for the former calculation.²⁷ Not surprisingly, loss of a proton from *syn*-**28-H**⁺ to the solvent is uphill by 11.8 kcal/mol, while loss of a proton to CO₃²⁻ to give HCO₃⁻ is strongly downhill by 18.2 kcal/mol. Attempts to locate transition states for deprotonations and protonations of these species and others shown later (Figure 8; INT1-H⁺ → **25**, INT3-H⁺ → **24**) were unsuccessful since the kinetic barrier to deprotonation should be very small. Deprotonation of **28-H**⁺ by solvent is unfavorable; however, if *stoichiometric* CO₃²⁻ were available in solution, only **28** can be present. The solubility of Na₂CO₃ in anhydrous MeOH is known to be negligible,²⁸ and our own measurements in TFE (shake-flask method) indicate a solubility of approximately 0.05 M. Compared to the concentration of chloroketone in the reaction (1.4 M), nearly 4% of base may be available in solution at a given time, raising the possibility that either **28** or **28-H**⁺ may serve as reactive species. Because the kinetics of both the formation of **28-H**⁺ and its deprotonation to give **28** in the presence of a mostly heterogeneous base is unknown, it seemed prudent to consider the intermediacy of both *syn*-**28-H**⁺ and *syn*-**28**.

First, the reaction of oxyallyl cation *syn*-**28** with *N*-methylskatole was examined using DFT. Two pathways were found as shown in Figure 8. The first, shown in black, allows

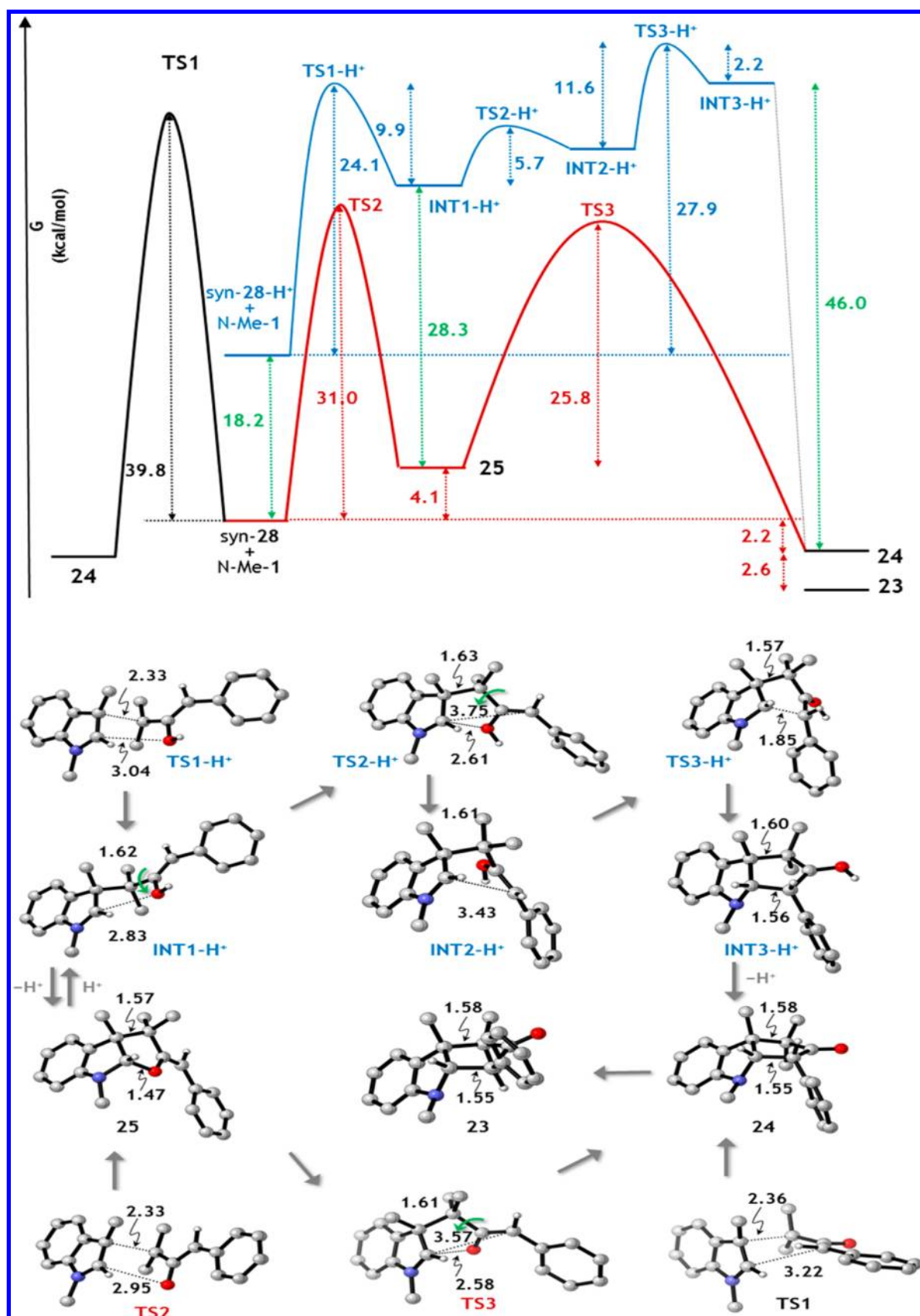


Figure 8. DFT calculated (B3LYP-D3/6-311++G**/CH₃OH) free energy profiles for reaction of N-methylskatole with oxyallyl cation *syn*-28 (black and red pathways) and hydroxyallyl cation *syn*-28-H⁺ (blue pathway), and calculated structures of transition states, intermediates, and products. Free energy differences are in kcal/mol, and distances are in Å. Numbers in green are free energy differences between the indicated protonated species plus CO₃²⁻ and the corresponding deprotonated species plus HCO₃⁻. Other than the two C–H bonds that define the stereochemistry of formation of the second C–C bond, all other C–H hydrogen atoms are omitted for clarity.

direct formation of **24** via a concerted but very unsymmetrical **TS1**, and the second, shown in red, involves stepwise formation of *O*-bound intermediate **25** via **TS2**, with subsequent rearrangement to product **24** via **TS3**. While both pathways involve high-energy transition states, the latter is the lower energy path, consistent with experimental observation of *O*-bound intermediate **25**. Transformation of **25** to **24** occurs via **TS3**, in which dissociation of the C–O bond in **25** is accompanied by directional rotation as shown by the curved green arrow to afford the relative stereochemical configuration obtained during formation of the second C–C bond in **24**. Final epimerization of **24** to **23** is predicted to be downhill by 2.6 kcal/mol, consistent with the observed thermodynamics of the overall reaction. For completeness, the analogous pathway for regioisomeric addition of *syn*-**28** to *N*-methylskatole was located; the corresponding energy of this **TS2** lies 5.7 kcal/mol higher than that shown in Figure 8. DFT correctly predicts formation of the *O*-bound intermediate and both the regiochemistry and stereochemistry of addition, starting from oxyallyl cation *syn*-**28**. However, earlier concerns about the insolubility of the added base raised the possibility that the reaction may flow not from *syn*-**28** but rather from its protonated analogue *syn*-**28-H**⁺.

To evaluate this possibility using DFT, reaction of the protonated hydroxyallyl cation *syn*-**28-H**⁺ with *N*-methylskatole was also examined, and the resultant lowest energy reaction profile is shown as the blue pathway in Figure 8. Initial reaction of *syn*-**28-H**⁺ with *N*-methylskatole proceeds via **TS1-H**⁺ to give **INT1-H**⁺ (identical to **29** in Scheme 1) in which the first C–C bond is formed and there is a long, presumably weak, C⋯OH interaction. At this stage, kinetically facile loss of a proton (*vide supra*) can afford the experimentally observed intermediate **25**, so it is perhaps not surprising that, in the presence of excess Na₂CO₃, a buildup of **25** is observed. It is notable that the activation free energy for formation of protonated **25** (**INT1-H**⁺) from the hydroxyallyl cation *syn*-**28-H**⁺ and *N*-methylskatole is only 24.1 kcal/mol, which is significantly lower than the 31.0 kcal/mol required for the direct formation of **25** from oxyallyl cation *syn*-**28** (Figure 8). Consequently, if *syn*-**28** and *syn*-**28-H**⁺ are both present in methanol under these conditions, the reaction of *syn*-**28-H**⁺ with the indole is predicted to be faster. In addition, the subsequent reaction of **INT1-H**⁺ to give **INT3-H**⁺, which is the *O*-protonated form of **24**, also has a considerably lower overall activation free energy than does the unprotonated analogue (Figure 8). Breaking the C–O bond in **INT1-H**⁺ is facilitated by protonation, allowing dissociation via a low energy **TS2-H**⁺ to give **INT2-H**⁺. Continued elongation of the C–O distance, with directional rotation as shown by the curved green arrow (Figure 8) via **TS3-H**⁺ leads to **INT3-H**⁺ with the correct relative stereochemistry resulting from construction of the second C–C bond. Transition states for direct formation of either species **INT2-H**⁺ or **INT3-H**⁺ from starting materials could not be located.

Proton loss from the reaction of **INT3-H**⁺ with CO₃²⁻ is strongly downhill to give **24**, so consumption of protons by Na₂CO₃ appears to be essential to drive the overall reaction by this pathway. It is also noteworthy that the blue pathway shown in Figure 8 is *proton-catalyzed* and that inefficient or reversible consumption of protons by an added base may still allow this pathway to occur even if only small concentrations of *syn*-**28-H**⁺ are present.

Thus, while a pathway for formation of product **24** from oxyallyl cation *syn*-**28** is available, our DFT calculations predict that it is a higher energy route than that emanating from the hydroxyallyl cation *syn*-**28-H**⁺. As mentioned above, divergent reactivity between oxyallyl and hydroxyallyl cations was also previously observed by Harmata and Schreiner.¹⁸ It seems likely that *unless oxyallyl cations are generated by stoichiometric, homogeneous, strong bases, the participation of hydroxyallyl cations as competitive reagents cannot be automatically excluded.*

CONCLUSION

The dearomatization of the C2/C3 double bond of 3-substituted indoles with α -haloketones has been reported. Both high efficiency and high diastereocontrol were observed in the majority of cases. DFT calculations suggest that the preferred mechanism for the formal cycloaddition may proceed via hydroxyallyl cations rather than the corresponding oxyallyl cations. *O*-Alkylated intermediates are initially formed, followed by isomerization to the observed products. The synthetic potential of this dearomatization process was demonstrated by concise syntheses of the core structures of vincorine, isocorymine, and aspidophylline A. With an eye toward targeting malagashanine, efforts are ongoing in our laboratory to obtain regioisomeric lactone **37**.

GENERAL PROCEDURE

To a TFE (0.18 mL) solution of **1** (40 mg, 0.18 mmol) and **2** (30 mg, 0.25 mmol) was added Na₂CO₃ (28 mg, 0.27 mmol). The heterogeneous reaction mixture was stirred at 40 °C until the reaction was judged complete as determined by thin layer chromatographic analysis. The mixture was filtered through a short pad of Celite and washed with 5 mL of EtOAc. The filtrate was concentrated *in vacuo*, and the residue was purified via silica gel column chromatography (3% EtOAc/hexane) to afford **3** as a colorless solid.

ASSOCIATED CONTENT

Supporting Information

Experimental details and characterization of all new compounds, CIF files, selected NOESY, HMBC, HMQC, DEPT data, details of DFT calculations, final geometry coordinates for all calculated structures, and larger scale graphics of Figures 7–8. This material is available free of charge via the Internet at <http://pubs.acs.org>.

AUTHOR INFORMATION

Corresponding Authors

jimmy.wu@dartmouth.edu

russell.p.hughes@dartmouth.edu

Notes

The authors declare no competing financial interest.

ACKNOWLEDGMENTS

Dedicated to our colleagues Professor David M. Lemal and Professor Thomas A. Spencer in celebration of their 80th birthdays. This work was supported in part by Dartmouth College. We thank Professors David M. Lemal, Peter A. Jacobi, and Gordon W. Gribble for useful discussions. We also thank Dr. Richard J. Staples (Michigan State University) for determination of X-ray structures and Wayne Casey (Dartmouth College) for assistance with NMR spectroscopy.

REFERENCES

- (1) Roche, S. P.; Porco, J. A., Jr. *Angew. Chem., Int. Ed.* **2011**, *50*, 4068–4093.
- (2) (a) Wu, Q. F.; Zheng, C.; You, S. L. *Angew. Chem., Int. Ed.* **2012**, *51*, 1680–1683. (b) Kimura, M.; Futamata, M.; Mukai, R.; Tamaru, Y. *J. Am. Chem. Soc.* **2005**, *127*, 4592–4593. (c) Trost, B. M.; Quancard, J. J. *J. Am. Chem. Soc.* **2006**, *128*, 6314–6315. (d) Wu, Q. F.; He, H.; Liu, W. B.; You, S. L. *J. Am. Chem. Soc.* **2010**, *132*, 11418–11419. (e) Kagawa, N.; Malerich, J. P.; Rawal, V. H. *Org. Lett.* **2008**, *10*, 2381–2384.
- (3) Lin, A.; Yang, J.; Hashim, M. *Org. Lett.* **2013**, *15*, 1950–1953.
- (4) Wu, K.; Dai, L. X.; You, S. L. *Org. Lett.* **2012**, *14*, 3772–3775.
- (5) (a) Austin, J. F.; Kim, S.-G.; Sinz, C. J.; Xiao, W.-J.; MacMillan, D. W. C. *Proc. Natl. Acad. Sci. U.S.A.* **2004**, *101*, 5482–5487. (b) Jones, S. B.; Simmons, B.; MacMillan, D. W. C. *J. Am. Chem. Soc.* **2009**, *131*, 13606–13607. (c) Horning, B. D.; MacMillan, D. W. C. *J. Am. Chem. Soc.* **2013**, *135*, 6442–6445.
- (6) (a) Zhang, L. *J. Am. Chem. Soc.* **2005**, *127*, 16804–16805. (b) Repka, L. M.; Ni, J.; Reisman, S. E. *J. Am. Chem. Soc.* **2010**, *132*, 14418–14420. (c) Kawano, M.; Kiuchi, T.; Negishi, S.; Tanaka, H.; Hoshikawa, T.; Matsuo, J.; Ishibashi, H. *Angew. Chem., Int. Ed.* **2013**, *52*, 906–910. (d) Zhang, G.; Huang, X.; Li, G.; Zhang, L. *J. Am. Chem. Soc.* **2008**, *130*, 1814–1815. (e) Martin, D.; Vanderwal, C. D. *J. Am. Chem. Soc.* **2009**, *131*, 3472–3473. (f) Robertson, F. J.; Kenimer, B. D.; Wu, J. *Tetrahedron* **2011**, 4327–4332.
- (7) (a) Jones, S. B.; Simmons, B.; Mastracchio, A.; MacMillan, D. W. C. *Nature* **2011**, *475*, 183–188. (b) Magnus, P.; Gallagher, T.; Brown, P.; Huffman, J. C. *J. Am. Chem. Soc.* **1984**, *106*, 2105–2114. (c) Kuehne, M. E.; Seaton, P. J. *J. Org. Chem.* **1985**, *50*, 4790–4796. (d) Wright, C. W. *Nat. Prod. Rep.* **2010**, *27*, 961–968. (e) Zu, L.; Boal, B. W.; Garg, N. K. *J. Am. Chem. Soc.* **2011**, *133*, 8877–9. (f) Zhang, M.; Huang, X.; Shen, L.; Qin, Y. *J. Am. Chem. Soc.* **2009**, *131*, 6013–6020. (g) Zi, W.; Xie, W.; Ma, D. J. *J. Am. Chem. Soc.* **2012**, *134*, 9126–9129. (h) Horning, B. D.; MacMillan, D. W. C. *J. Am. Chem. Soc.* **2013**, *135*, 6442–6445. (i) Li, Q.; Li, G.; Ma, S.; Feng, P.; Shi, Y. *Org. Lett.* **2013**, *15*, 2601–2603. (j) Hugel, G.; Cartier, D.; Levy, J. *Tetrahedron Lett.* **1989**, *30*, 4513–4516. (k) Dethe, D. H.; Erande, R. D.; Ranjan, A. *J. Org. Chem.* **2013**, *78*, 10106–10120.
- (8) (a) Wenkert, E.; Moeller, P. D.; Piettre, S. R. *J. Am. Chem. Soc.* **1988**, *110*, 7188–7194. (b) Cai, Q.; You, S. L. *Org. Lett.* **2012**, *14*, 3040–3043. (c) Biolatto, B.; Kneeteman, M.; Paredes, E.; Mancini, P. M. E. *J. Org. Chem.* **2001**, *66*, 3906–3912. (e) Hsieh, M.; Rao, P. D.; Liao, C. C. *Chem. Comm.* **1999**, 1441–1442.
- (9) (a) England, D. B.; Kuss, T. D. O.; Keddy, R. G.; Kerr, M. A. *J. Org. Chem.* **2001**, *66*, 4704–4709. (b) Bajtos, B.; Yu, M.; Zhao, H.; Pagenkopf, B. L. *J. Am. Chem. Soc.* **2007**, *129*, 9631–9634. (c) Xiong, H.; Xu, H.; Liao, S.; Xie, Z.; Tang, Y. *J. Am. Chem. Soc.* **2013**, *135*, 7851–7854. (d) Barluenga, J.; Tudela, E.; Ballesteros, A.; Tomas, M. J. *J. Am. Chem. Soc.* **2009**, *131*, 2096–2097. (e) Lian, Y.; Davies, H. M. L. *J. Am. Chem. Soc.* **2010**, *132*, 440–441.
- (10) Han, X.; Li, H.; Hughes, R. P.; Wu, J. *Angew. Chem., Int. Ed.* **2012**, *51*, 10390–10393.
- (11) Han, X.; Wu, J. *Angew. Chem., Int. Ed.* **2013**, *52*, 4637–4640.
- (12) (a) Harmata, M. *Chem. Commun.* **2010**, 46, 8886–8903. (b) Harmata, M. *Chem. Commun.* **2010**, 46, 8904–8922. (c) Harmata, M. *Adv. Synth. Catal.* **2006**, *348*, 2297–2306. (d) Lohse, A. G.; Hsung, R. P. *Chem.—Eur. J.* **2011**, *17*, 3812–3822.
- (13) (a) Tang, Q.; Chen, X.; Tiwari, B.; Chi, Y. *Org. Lett.* **2012**, *14*, 1922–1925. (b) Vander Wal, M. N.; Dilger, A. K.; MacMillan, D. W. *Chem. Sci.* **2013**, *4*, 3075–3079.
- (14) Giese, S.; Kastrup, L.; Stiens, D.; West, F. G. *Angew. Chem., Int. Ed.* **2000**, *39*, 1970–1973.
- (15) Marx, V. M.; Burnell, D. J. *J. Am. Chem. Soc.* **2010**, *132*, 1685–1689.
- (16) Fujita, M.; Oshima, M.; Okuno, S.; Sugimura, T.; Okuyama, T. *Org. Lett.* **2006**, *8*, 4113–4116.
- (17) (a) Hayakawa, Y.; Yokoyama, K.; Noyori, R. *J. Am. Chem. Soc.* **1978**, *100*, 1799–1806. (b) Corriu, R. J. P.; Moreau, J. J. E.; Pataud-Sat, M. *J. Org. Chem.* **1990**, *55*, 2878–2884.
- (18) Harmata, M.; Huang, C.; Rooshenas, P.; Schreiner, P. R. *Angew. Chem., Int. Ed.* **2008**, *47*, 8696–8699.
- (19) (a) Bevan, C. W. L.; Patel, M. B.; Rees, A. H.; Harris, D. R.; Marshak, M. L.; Mills, H. H. *Chem. Ind.* **1965**, *14*, 603–604. (b) Vercauteren, J.; Massiot, G.; Le Men-Olivier, L.; Levy, J.; Delaude, C. *Bull. Soc. Chim. Fr.* **1982**, 9–10 (pt. 2), 291–296.
- (20) (a) Lee, C.; Yang, W.; Parr, R. G. *Phys. Rev. B* **1988**, *37*, 785–789. (b) Becke, A. D. *J. Chem. Phys.* **1993**, *98*, 5648–5652. (c) Becke, A. D. *J. Chem. Phys.* **1993**, *98*, 1372–1377. (d) Stephens, P. J.; Devlin, F. J.; Chabalowski, C. F.; Frisch, M. J. *J. Phys. Chem.* **1994**, *98*, 11623–11627. (e) Andersson, M. P.; Uvdal, P. *J. Phys. Chem. A* **2005**, *109*, 2937–2941.
- (21) (a) Dunning, T. H.; Hay, P. J. In *Modern Theoretical Chemistry, Vol. 4: Applications of Electronic Structure Theory*; Schaefer, H. F., III, Ed.; Plenum: NY, 1977. (b) Hay, P. J.; Wadt, W. R. *J. Chem. Phys.* **1985**, *82*, 270–283. (c) Hay, P. J.; Wadt, W. R. *J. Chem. Phys.* **1985**, *82*, 299–310. (d) Wadt, W. R.; Hay, P. J. *J. Chem. Phys.* **1985**, *82*, 284–298.
- (22) *Jaguar*, versions 7.0–7.9, Schrödinger, L. L. C., New York, NY, 2007–2012.
- (23) (a) Grimme, S.; Antony, J.; Ehrlich, S.; Krieg, H. *J. Chem. Phys.* **2010**, *132*, 154104. (b) Goerigk, L.; Grimme, S. *Phys. Chem. Chem. Phys.* **2011**, *13*, 6670–6688.
- (24) Lopchuk, J. M.; Hughes, R. P.; Gribble, G. W. *Org. Lett.* **2013**, *15*, 5218–5221.
- (25) (a) Tannor, D. J.; Marten, B.; Murphy, R.; Friesner, R. A.; Sitkoff, D.; Nicholls, A.; Honig, B.; Ringnalda, M.; Goddard, W. A. *J. Am. Chem. Soc.* **1994**, *116*, 11875–11882. (b) Marten, B.; Kim, K.; Cortis, C.; Friesner, R. A.; Murphy, R. B.; Ringnalda, M. N.; Sitkoff, D.; Honig, B. *J. Phys. Chem.* **1996**, *100*, 11775–11788.
- (26) Bettinger, H. F. *Angew. Chem., Int. Ed.* **2010**, *49*, 670–671.
- (27) Kelly, C. P.; Cramer, C. J.; Truhlar, D. G. *J. Phys. Chem. B* **2007**, *111*, 408–422.
- (28) Ellingboe, J. L.; Runnels, J. H. *J. Chem. Eng. Data* **1966**, *11*, 323–324.